Published in final edited form as:
J Phys Chem C Nanomater Interfaces. 2011 November 18; 115(32): . doi:10.1021/jp2042526.

Unveiling N-protonation and anion-binding effects on Fe/N/C-catalysts for O_2 reduction in PEM fuel cells

Juan Herranz[a], **Frédéric Jaouen**[a,*], **Michel Lefèvre**[a], **Ulrike I. Kramm**[a,b], **Eric Proietti**[a], **Jean-Pol Dodelet**[a], **Peter Bogdanoff**[b], **Sebastian Fiechter**[b], **Irmgard Abs-Wurmbach**[c], **Patrick Bertrand**[d], **Thomas M. Arruda**[e], and **Sanjeev Mukerjee**[e]

[a]Institut National de la Recherche Scientifique, Énergie, Matériaux et Télécommunications, Varennes, Québec, J3X 1S2, Canada

[b]Helmholtz-Zentrum Berlin für Materialien und Energie Lise-Meitner-Campus, Institute for solar fuels and energy storage (E-I-6) Hahn-Meitner-Platz 1, D-14109, Berlin, Germany

[c]Technical University Berlin, Faculty VI, Ackerstrasse 76, D-13355, Berlin, Germany

[d]Université Catholique de Louvain, Institut de la matière condensée et des nanosciences Croix-du-sud 1, 1348 Louvain-la-neuve, Belgium

[e]Northeastern University, Department of Chemistry and Chemical Biology, Boston, MA-02115, U.S.A

Abstract

The high cost of proton-exchange-membrane fuel cells would be considerably reduced if platinumbased catalysts were replaced by iron-based substitutes, which have recently demonstrated comparable activity for oxygen reduction, but whose cause of activity decay in acidic medium has been elusive. Here, we reveal that the activity of Fe/N/C-catalysts prepared through a pyrolysis in NH_3 is mostly imparted by acid-resistant FeN_4-sites whose turnover frequency for the O_2 reduction can be regulated by fine chemical changes of the catalyst surface. We show that surface N-groups protonate at pH 1 and subsequently bind anions. This results in decreased activity for the O_2 reduction. The anions can be removed chemically or thermally, which restores the activity of acid-resistant FeN_4-sites. These results are interpreted as an increased turnover frequency of FeN_4-sites when specific surface N-groups protonate. These unprecedented findings provide new perspective for stabilizing the most active Fe/N/C-catalysts known to date.

Keywords

Electrocatalysis; non precious metal; durability; degradation; acid; oxygen reduction

1. Introduction

Proton-Exchange-Membrane Fuel Cells (PEMFCs) are well-suited electrical power generators for portable and automotive applications due to their high efficiency, high power density and low operating temperature. While this technology is being deployed in niche

*corresponding author: jaouen@emt.inrs.ca.

Supporting information **available:** Effect of immersion time on surface areas and N1s spectra of acid-washed catalysts; activity recovery by re-heat-treatment after acid-washing in 0.1 M $HClO_4$; identification of surface species by XPS and TG-MS upon acid washing in 0.1 M $HClO_4$; derivation of equations to analyze the Boehm titration experiment. This information is available free of charge via the internet at http://pubs.acs.org.

markets, its cost remains prohibitive for widespread commercialization, especially for automotive propulsion. Based on a production volume of 500,000 automotive PEMFC units, it is predicted that the Pt-based catalyst would account for half of the PEMFC-stack cost.[1] Due to the slow kinetics of the Oxygen Reduction Reaction (ORR), 90% of the platinum in the latest H_2/air PEMFCs is needed at the cathode.[2] Hence, the development of non-precious metal catalysts with high ORR-activity and durability has become a major focus in recent years.

After it was first discovered that cobalt-phthalocyanine was active toward the ORR,[3] progress continued with the finding that a heat-treatment above 600°C increased the activity of catalysts based on metal-N_4 macrocycles.[4] It was later reported that similar activity could be achieved by heat-treating catalyst precursors made simply of (i) a transition metal salt (ii) nitrogen and (iii) carbon.[5-7] Among the transition metals in period 4, iron produces the most active catalysts in acidic medium, referred to as Fe/N/C-catalysts because of the spectroscopic evidence of FeN_4-moieties.[8-12] In 2009, our group reported on an innovative synthesis that remarkably increased the activity of Fe/N/C-catalysts, but not their durability.[13] Stable currents in PEMFC for less active Fe/N/C-based cathodes have, however, been demonstrated for 60-200 h at 0.5 V [6, 14] and recently for 280-600 h at 0.4 V.[15-16] Therefore, bridging the gap between the attributes responsible for high activity and high durability has become the main challenge facing Fe/N/C-catalysts.[17]

The present work reveals that (i) some FeN_4-sites located on the catalyst's top surface are structurally stable in acidic medium, (ii) specific N-groups on the catalyst surface (and not involved in Fe-coordination) protonate in acidic medium and bind anions, resulting in activity decay, and (iii) these bound-anions can be removed thermally or chemically, which restores the activity of the acid-resistant FeN_4-sites.

The time scale for anion binding, and therefore for activity decay, greatly depends on the anion pervasiveness in the electrolyte; slow in a polymer electrolyte, fast in a liquid electrolyte. These findings are unprecedented and disprove assertions that the activity decay of Fe/N/C-catalysts in acidic medium is entirely ascribed to irreversible demetallation.[18,19]

2. Experimental Methods

2.1. Sample preparation

2.1.1. Synthesis of original catalyst (O-catalyst) by the impregnation method—

A carbon black having a surface area of 71 m^2g^{-1} was impregnated in de-ionized water with $iron^{II}$ acetate (0.2 wt% Fe). After stirring for 3 h, the powder was dried overnight in air at 80°C. The resulting powder was ground, placed in a quartz boat and heat-treated at 950°C under a flow of NH_3 for the duration necessary to reach a weight loss of 30-35 w %, corresponding to the maximum microporous surface area and activity.[20-21] Details of the heat-treatment procedure are found in Ref.20. Several batches of this O-catalyst were prepared, with ORR activity at 0.8 V vs RHE ranging from 2.3 to 2.8 A g^{-1}, as measured at pH 1 with a rotating disk electrode.

2.1.2. Acid-washing a catalyst—

Hundred milligrams of catalyst was immersed in 50 mL of a pH 1 H_2SO_4-solution to which 0.5 mL ethanol was added to help dispersion. The solution was stirred at room temperature for a set time, ranging from 5 min to 100 h. Then, the powder was filtered, rinsed with deionized water and dried at 80°C in air. The resulting powder is called an *acid-washed catalyst* (AW-catalyst).

2.1.3. Catalyst re-heat-treatment—The re-heat-treatment of acid-washed catalysts was performed in argon for 1 h at a set temperature, ranging from 200 to 950°C. Such samples are labelled RHT-catalysts.

2.1.4. Preparation of test precursor—A test precursor, free of catalytic sites, but meeting all requirements to form catalytic sites upon heat-treatment in argon, was prepared by (i) heat-treating the pristine carbon black (the same used to prepare the original catalyst) in NH_3 at 950°C until the maximum microporous surface area was reached (Ref.20), (ii) impregnating this NH_3-heat-treated carbon black with iron acetate (0.16 wt % Fe) and (iii) drying the resulting powder.

2.2. Activity and durability measurements

2.2.1. Activity measurement in RDE at room temperature—The electrolyte was a pH 1 H_2SO_4-solution. An ink was prepared by mixing 10 mg of catalyst, 95 μL of a 5 wt% Nafion solution and 350 μL of ethanol. The catalyst loading was 0.8 mg cm^{-2}. The potential was scanned at 10 mV s^{-1} between -0.25 and 0.75 V vs. a saturated calomel electrode (SCE). In the O_2-saturated electrolyte, the first cycle was performed without rotation and the second with an electrode rotation of 1500 rpm. Then, the electrolyte was N_2-saturated and one more cycle was recorded. After correction of the 1500 rpm-cycle for all non-ORR currents, the curve of the ORR current vs. potential was obtained. The scalar needed to convert from SCE to RHE was obtained from the voltage between the SCE reference electrode and a Pt-wire in the H_2-saturated electrolyte (experimentally at pH 1, mV vs RHE = mV vs SCE + 310 ± 5 mV). Then, the current-potential curve was corrected for diffusion-limitation using the Koutecky-Levich equation. The assessment of the kinetic ORR-activity, I_k (A cm^{-2}_{geom}), was made at 0.8 V vs. RHE and based on the negative-going scan of the corrected curve. For each catalyst, the activity reported is an average based on three electrodes.

2.2.2. Activity measurement in PEMFC at 80°C—The membrane electrode assembly (MEA) was prepared as described in the supporting information of Ref. 13. The cathode catalyst loading was 1 mg cm^{-2}. Pt-on-carbon was used at the anode and the membrane was Nafion 117. The fuel cell temperature was 80°C, and the humidifiers were set to 105°C (H_2) and 90°C (O_2) to reach 100 % relative humidity. The gauge pressure was the same for the anode and cathode sides and was either 1 bar (activity tests) or 2 bars (durability tests). The fuel cell and humidifiers were brought to temperature with N_2 flows. When the set temperatures were reached, N_2 was switched to pure O_2 and H_2 and the polarization curve was recorded without break-in, using a scan rate of 0.5 mV s^{-1}. The assessment of the kinetic ORR-activity, I_k (A cm^{-2}_{geom}), was made at 0.8 V after correction of the polarization curve for ohmic drop. When the kinetically controlled region of that curve did not include the voltage of 0.8 V, then the kinetic activity at 0.8 V was assessed by extrapolation of the Tafel slope.

2.2.3. Definition of mass activity and turnover frequency—Since the kinetic activity of a porous electrode is a function of the catalyst loading, we report instead the mass activity (A/g) at 0.8 V, defined by [13]

$$I_m = -I_k/m \quad (1)$$

Where I_k (A cm^{-2}_{geom}) is defined negative for a reduction reaction and m is the catalyst loading (g cm^{-2}_{geom}). Mass activities are reported in the results section of the present work. At a more detailed level however, the mass activity of a catalyst is proportional to the

mathematical product of the density of active sites with the average turnover frequency for the ORR of these active sites,[21]

$$I_m = \mathrm{SD} \times \mathrm{ATF} \times e \quad (2)$$

Where SD is the site density (sites g^{-1}), ATF is the average turnover frequency of all active sites (electrons per site per second) at 0.8 V and e is the electric charge of a single electron ($1.6\ 10^{-19}$ C). Currently, there is no direct method to experimentally determine SD in Fe/N/C-catalysts. Therefore, values of I_m are reported throughout the results section. The concept of turnover frequency is used solely in the discussion section of the present work, once it has been shown that the SD of the O-catalyst is unchanged following two or more acid washings. Since the dispersed molecular active sites in Fe/N/C-catalysts do not define a surface area, the concept of turnover frequency is convenient to report their specific electrocatalytic activity. In contrast, the specific activity of Pt-based catalysts can be reported either in the form of turnover frequency or of current per surface area of platinum.

2.2.4. Durability measurement in H_2/O_2 PEMFC at 80°C—After an initial activity-measurement, the cell voltage was held either at open-circuit (OCV-Mode) with H_2/O_2 gases at anode/cathode, or 0.5 V (0.5V-Mode(H_2/N_2) or 0.5V-Mode(H_2/O_2)). For the OCV-Mode and 0.5V-Mode(H_2/N_2), the polarization curves for the activity assessment under H_2/O_2 were measured between OCV and 0.78 V to minimize the Faradaic charge during durability tests, while for the 0.5V-Mode(H_2/O_2) they were measured between OCV and 0.0 V after the cell was held at OCV for 30 min.

2.3 Ex-situ characterization of catalysts

2.3.1. X-ray photoelectron spectroscopy (XPS)—X-ray photoelectron spectroscopy was performed using a VG Escalab 200i instrument. The x-ray source was the Al K_α line (1486.6 eV). Narrow scans were performed for the C_{1s}, N_{1s}, O_{1s}, and S_{2p} core levels. The pass energy was 20 eV and the energy increment 100 meV. Quantification of the elements was performed using Casa software.

2.3.2. Mössbauer spectroscopy—Mössbauer experiments were performed at the Mineralogical Department of the TU Berlin using a ^{57}Co/Rh-source. Each spectrum was recorded at room temperature with a 1024 multichannel analyzer equipped with a constant electronic drive system with triangular reference waveform. All spectra were calibrated using the sextet spectrum of an α-Fe foil (purity > 99.99%) and the known positions of its absorption lines. Furthermore, the centre of symmetry of this spectrum was taken as zero-velocity. All investigated catalysts were prepared using ^{57}Fe-enriched iron acetate (>95% ^{57}Fe). The graphs present the absorption intensity (Abs), calculated from the transmission spectra by the equation $Abs = -\frac{(Trans_{Max} - Trans(\nu))}{Trans_{Max}} \cdot 100$; where $Trans_{Max}$ is the maximum intensity of the transmitted signal.

2.3.3. Time-of-Flight Secondary Ion Mass Spectrometry (ToF-SIMS)—The surface composition of the catalysts was analyzed by ToF-SIMS (Charles-Evans and Associates) using Ga^+ 15 keV primary ions with a resolution of 10000 for Si on a Si wafer. For the samples, a mass resolution (m/Δm) of about 4000 at the Si mass (m) was obtained. For the analysis, the catalysts were deposited on an Ag foil pre-coated with conductive glue. Four regions were analyzed for each sample and a mean value was obtained. A seven keV post-acceleration was used with the 0-1000 amu range analysis. The delivered dose was below 10^{12} ions/cm^2, remaining therefore in the static SIMS range.

2.3.4. Extended X-ray Absorption Fine-Structure (EXAFS)—Sample vials containing the catalyst powders were transferred to an argon-filled glove box for sample preparation. Each sample was prepared by placing approximately 50 mg of catalyst powder between two pieces of polyamide tape (3M Corporation) to form a catalyst pouch. The edges of pouch were sealed off with more polyamide tape and the pouches were stored in argon in an air-tight, resealable polyethylene bag for transport. X-ray absorption spectroscopy measurements were performed at X3-B at the National Synchrotron Light Source at Brookhaven National Laboratory, Upton, NY. Fluorescence mode X-ray absorption spectroscopy was collected over a range of -200 eV to 800 eV with respect to the Fe k-edge (7112 eV). Data acquisition was such that data points were measured at 5 eV increments (-200 to -50 eV, one-second integration time), followed by 0.5 eV increments (-50 to 50 eV, 2-second integration) and 5 eV increments (50–800 eV, 3-second integration). X-ray detection was achieved using gas ionization detectors filled with 100% N_2 in I_0 (incident beam), I_t (transmitted beam) and I_{ref} (reference). Fluorescence x-rays (I_f) were detected using a 13 element Ge detector (Canberra). The Fe/N/C samples were placed between I_0 and I_t while an Fe foil (5 μm, Goodfellow) was located between I_t and I_{ref} in order to track changes to the beam energy over the course of the experiment. X3-B employs a double crystal Si(111) monochromator with a Bragg angle range of 8.5-35 degrees, located 16.5 m from the bending magnet source. A minimum of three scans was collected for each sample due to the low concentration of Fe in the samples. The EXAFS-spectra were Fourier-Transformed using the relationship: $\chi(R)=\frac{1}{\sqrt{2\pi}}\int_{k_{\min}}^{k_{\max}} k^n \chi(k) e^{i2kR} dk$; where k_{min} and k_{max} are the FT window (from 2 to approximately 12 $Å^{-1}$) and χ(k) is the normalized EXAFS.

2.3.5. Acid-base properties of the surface—A classical acid-base titration of the original catalyst was performed using 500 mg of original catalyst in suspension in 25 mL of de-ionized water. The titrant was a 0.01M $HClO_4$ solution.

A Boehm type of titration was also performed on the original catalyst. Eleven aqueous solutions with pH ranging from 1 to 11 were prepared using de-ionized water and H_2SO_4 or NaOH. For each solution, an aliquot of 10 mL was taken and its initial pH measured. Then, 20 mg of the original catalyst was added and the final pH was measured after 20 min of stirring.

3. Results

For clarity, the catalysts in this work are categorized using three descriptors: original, acid-washed and re-heat-treated. The original catalyst (O-catalyst) was prepared as described in the Experimental Methods. Acid-washed catalysts (AW-catalysts) are samples of the O-catalyst that were immersed into an H_2SO_4-solution of pH 1 while re-heat-treated catalysts (RHT-catalysts) are AW-catalysts that underwent a subsequent heat-treatment in argon (see Experimental Methods). The ORR-activity was assessed in PEMFC and rotating-disk-electrode (RDE) based on the mass-activity, I_m, measured at 0.8 V vs. a Reversible Hydrogen Electrode (RHE); henceforth referred to as *the activity*.

3.1. Durability in PEMFC for the original catalyst

The poor durability of Fe/N/C-catalysts has often been imputed to minor amounts of H_2O_2 released during the ORR.[22] To investigate this assertion, three durability tests were performed (Fig.1). The first involves holding the cell at open circuit voltage under H_2/O_2 for a total of 100 hours while taking activity measurements at various times (OCV-Mode). The second and third are similar but the voltage is 0.5 V and gases are either H_2/N_2 or H_2/O_2, respectively. For the OCV-Mode and 0.5V-Mode(H_2/N_2), O_2 reduction occurs only during

each of the short activity measurements. For the O-catalyst, the activity decay in PEMFC under OCV-Mode (empty circles), 0.5V-Mode(H_2/N_2) (empty squares) or 0.5V-Mode(H_2/O_2) (filled squares) is shown in Fig.1A. The fivefold larger decay under 0.5V-Mode(H_2/O_2) after 100 h is not commensurate with its 3,000-time larger ORR-Faradaic charge, which implies a ca 3,000 time larger cumulative production of H_2O_2 over 100 h (Fig.1B). Hence, H_2O_2 production during the ORR is not the only source of deactivation and it is also evident that a large activity-decay occurs even with minimized ORR-Faradaic charge (empty circles or empty squares in Fig. 1B).

To better understand activity decay without ORR, the O-catalyst powder was immersed in a pH 1 H_2SO_4-solution for 100 h, then filtered, rinsed and dried. The initial activity of this AW-catalyst is $1/20^{th}$ that of the O-catalyst (Fig.1, asterisk) and approximately equal to that of the O-catalyst after 50 h under OCV-Mode. This suggests that the activity-decay mechanism during the OCV-Mode in PEMFC may be similar to that during acid-washing in a pH 1 H_2SO_4-solution.

3.2. Effects of acid-washing (AW), re-heat-treatment (RHT) and multiple AW-RHT cycles

The effect of immersion time of the O-catalyst in a pH 1 H_2SO_4-solution on the activity of the resulting AW-catalysts was then investigated. Surprisingly, a mere five minutes is sufficient to reach the minimum activity, as measured by RDE (Fig.2A). The nitrogen content/bond-types and specific surface areas, two important parameters for Fe/N/C-catalysts, were unaffected upon immersion in acid solution (Supporting Figures S1A-B). However, after five minutes of immersion, only 30% of the Fe was leached (Fig.2B) while the activity decreased tenfold (Fig.2A). This disparity suggests that the activity decay may not be imputed solely to demetallation. This is evidenced by Fig.3A which shows the activity of nine aliquots of the same AW-catalyst after re-heat-treatment in argon at temperatures between 200 and 950°C. Notice how maximum activity recovery is reached at 300°C; a temperature that is much lower than the minimum 600°C needed to form new catalytic sites from Fe salt, N and C precursors.[7, 12, 23] To demonstrate the latter assertion, we prepared a test precursor free of catalytic sites, but that meets all requirements to form catalytic sites upon heat-treatment in argon (see Experimental Methods, section 2.1.4). This test precursor indeed shows ORR-activity only after a heat-treatment in argon above 600°C (Fig.3A, asterisks). Hence, the activity recovery observed between 200 and 300°C cannot be attributed to the creation of new sites. Instead, we attribute it to an increased ORR turnover frequency of catalytic sites that were already present in the AW-catalyst. From Fig.3A we may also conclude, however, that half of the activity decay is non-recoverable. The two different types of activity decay are defined as *Recoverable Activity Decay* (R-AD) and *Non-Recoverable Activity Decay* (NR-AD). The present paper focuses on the R-AD.

In addition to the Fe/N/C-catalyst discussed thus far, we verified that activity recovery by re-heat-treatment after acid-washing also works for a more active Fe/N/C-catalyst synthesized by the pore-filling method described in Ref.13. The remainder of this work focuses on the less active impregnation Fe/N/C-catalyst to avoid Fe-impurities coming from the ball-milling step of the pore-filling method.

To further our understanding of the R-AD observed in Fig.3A, the same AW- and RHT-samples were analysed using various techniques. X-ray photoelectron spectroscopy (XPS) of the AW-catalyst shows a peak at 166-170 eV that is ascribed to bisulfate-type sulfur (Fig. 4A).[24] The disappearance of this peak at 300°C coincides with activity recovery. The other S-peak (162-166 eV) originates from impurities in the as-received carbon black (labelled as *Carbon* in Fig.4A) and remains throughout. Furthermore, thermogravimetry and mass-spectrometry on the AW-catalyst also correlate the activity recovery with the removal of sulfur species between 200 and 340°C (Figs.4B-C). Lastly, time-of-flight secondary-ion

mass-spectrometry (Fig.4D) reveals that (i) HSO_4^- is detected on the AW-catalyst but removed by the heat-treatment in argon, (ii) a higher content of quaternary-N cation is detected on the AW-catalyst and (iii) some surface iron remains on the AW-catalyst. The above experiments were repeated using 0.1 M $HClO_4$ instead of 0.1 M H_2SO_4 for the acid-washing step. The results show strong similarities with those obtained using 0.1 M H_2SO_4 (Figs.S2-S3). The only difference is that upon re-heat-treatment, $HClO_4$ reacts with the carbon support at 150-350°C, releasing CO_2 (Fig.S3D) and forming chloride anions that are still bound on the surface at 400°C (Fig.S3A). These chloride anions leave the surface very slowly at 300°C but more rapidly at 700°C (Fig.S3C). The temperature needed for activity recovery upon a one-hour heat-treatment is 500°C (Fig.S2).

In conclusion, these data demonstrate that the activity recovery by re-heat-treatment in Ar coincides with the removal of anions. Anion binding during acid-washing implies the presence of positively-charged groups on the catalyst surface. Moreover, we can conclude that the ORR-activity is mostly imparted by strongly ligated Fe-ions at the surface since the initial activity measured in RDE of the pristine carbon black (no iron acetate impregnated) heat-treated at 950°C in NH_3 is only 0.04 A g^{-1}; much lower than 2.8 A g^{-1} for the impregnation Fe/N/C-catalyst. In addition, acid-washing the NH_3 heat-treated carbon black further decreases its activity to 0.008 A g^{-1}. Therefore, the presence of Fe imparts a factor 40-70 higher activity, be it in the as-synthesized or acid-washed state of the powder.

To further demonstrate that some Fe-ions resist acid-leaching while other Fe-species are leached mostly during the first acid-washing, several cycles of acid-washing and re-heat-treatment were performed (Fig.3B). It is expected that an O-catalyst that undergoes multiple acid-washing/re-heat-treatment cycles should have the same level of activity decay and recovery for each cycle, except for the NR-AD observed in the first cycle. Figure 3B precisely demonstrates this behaviour. After the fourth AW/RHT-cycle, the Fe bulk-content levels off to circa $1/4^{th}$ the Fe-content of the O-catalyst (Fig.3C). Moreover, for each cycle, the activity recovery is accompanied by the removal of bisulfate-type S from the surface of AW-catalysts while the N content remains constant (Fig.5). Also, for the AW-catalyst, there is quantitative agreement between the loss of 1.5 wt % observed in thermogravimetry (Fig. 4B) and the bisulfate-type S content of 0.12-0.15 at % (equivalent to 1.0-1.2 wt % HSO_4^-) measured by XPS (Fig.5A).

In order to gain knowledge on the nature of the Fe-species remaining after several AW/RHT cycles, Fe^{57} Mössbauer spectroscopy was performed on an AW-catalyst and a RHT-catalyst, both obtained from the fourth cycle of AW/RHT. Their spectra are nearly identical (Fig.6) and mostly characterized by doublets being characteristic for FeN_4-moieties.[11, 25]

If the acid-resistant FeN_4-moieties are the ORR-active sites in AW- and RHT-catalysts, how can the acid-washing affect their activity? Direct anion binding onto Fe-ions can be discarded for three reasons: (i) no coordination change of Fe-ions is detected by Mössbauer spectroscopy; (ii) no activity decay is observed after immersion of a RHT-catalyst in 0.1 M K_2SO_4 or 0.1 M KCl (note that a 0.1 M HCl aqueous solution, having the same counter-anion as a 0.1 M KCl solution, does result in the NR-AD mechanism for a RHT-catalyst); (iii) no significant difference in the 0-2 Å range is observed by Extended X-ray Absorption Fine-Structure between AW- and RHT-catalysts, which signifies that the first-shell coordination around Fe-ions was unmodified (Fig.7). Supporting these observations, a recent study has also reported that heat-treated Fe-phthalocyanine is not poisoned by anions, except by CN^- at pH 13.[26] Having discarded anion-binding to Fe-ions, the positively-charged sites necessary to explain anion retention upon acid-washing and rinsing could result from the protonation of surface functionalities having a basic character. Likely, these functionalities

on the surface of this particular Fe/N/C-catalyst prepared by pyrolysis in NH_3 may be N-functionalities.

3.3. Characteristics of the protonable N-functionalities and chemical reactivation of the catalyst

In order to obtain more information on the suspected basic N-groups on the catalyst surface, titration of the O-catalyst was performed with a 0.01 M $HClO_4$ solution (Fig.8A). We do not observe the typical shape expected for the titration curve of a weak base with well-defined pKa by a strong acid. The absence of a sharp decrease of pH at equivalence may be explained by the presence of different types of basic N-functionalities, characterized by a range of pKa values. If that is so, the basic groups with highest pKa would protonate at small volumes of titrant (high pH) while basic groups with lower pKa would protonate for larger volumes of titrant (low pH). This would forebode a classical behaviour of the titration curve.

Since a classical acid-base titration was unable to provide the desired information, it was then decided to use a “Boehm”-type titration which is more practical to estimate an average pKa-value, or pKa of the most frequently occurring basic groups. Aqueous solutions of a given initial pH, ranging from 1 to 13, were prepared. An aliquot of 20 mg of the O-catalyst was immersed in 10 mL of each of these solutions, and the final pH-values were measured. The curve of final vs. initial pH is presented in Fig.8B. The “Boehm” titration experiment was also modelized (see supporting information) and a calculated curve closely matching the experimental one is shown in Fig.8B (solid line). The curve was calculated for a concentration of protonable N-groups, B_0, of $7\ 10^{-4}$ mol L^{-1} and for an average pKa value of 6.5. Following an in-depth analysis of the model, the value $-\log(B_0)$ is read on the initial-pH axis at the inflection point of the experimental curve, while the final pH-value at the plateau is equal to $7 + 0.5 \log(B_0) + 0.5$ pKa. The above value for B_0 corresponds to $3.5 \cdot 10^{-4}$ mole of protonable N-groups per gram of catalyst, which in turn corresponds to 0.42 at %. Since about 2 at % N was detected by XPS for the O-catalyst (Fig.5C), it is concluded that about 20 % of all N-atoms may protonate. Furthermore, there is a maximum of 0.01 at % Fe involved in acid-resistant FeN_4-moieties (Fig.3C) and, consequently, only a maximum of 0.04 at % N involved in these FeN_4-moieties. This content is one-order-of-magnitude lower than that of protonable N-atoms (0.42 at %) for the presently investigated O-catalyst. The N-atoms involved in the FeN_4-moieties, as well as all other non-protonable N-atoms at pH 0-1, must therefore have a very low basicity (low pKa of conjugate acid), as mentioned in Ref. 27.

Therefore, the acid-washing affects the ORR-activity of acid-resistant FeN_4-moieties through protonation of specific basic N-functionalities, followed by instant anion-binding. One of the consequences for an AW-catalyst is that any strong base should react with its NH^+-groups (weak acids) to form N-atoms and H_2O. Simultaneously, anions previously bound to NH^+-groups by electrostatic interaction should diffuse away and be removed during the rinsing step. Therefore, chemical activity-recovery should be observed after an AW-catalyst is immersed in a strongly basic solution. This is shown in Fig.9A, where the ORR-activity following acid-washing, base-washing, filtration, rinsing and drying is equal to that measured after acid-washing followed by reheat-treatment at 300°C in argon. Subjecting the O-catalyst to base-washing alone resulted only in the NR-AD (not shown). As expected, chemical activity-recovery is also accompanied by the removal of the bisulfate-type S_{2p} signal (Fig.9B).

4. Discussion

The exact type of protonable N-groups present on the catalyst surface is not known, but possibilities may be narrowed down based on (i) the mean pKa-value of 6.5 obtained from Boehm titration and (ii) N_{1s} XPS-spectra (Fig. S1A). Pyridinic nitrogens are possible candidates since pyridine has a pKa of 5.2. Moreover, adding an amino-group in the ortho-position of pyridine, for instance, raises its pKa to 6.86.[28] In the N_{1s} XPS spectrum of the catalyst, the peak with the lowest binding energy is usually attributed (at least partially) to a pyridinic N-atom. Certainly, other nitrogen functionalities with pKa slightly above or below 6.5 are also possible. The case of pyridinic nitrogen is especially of interest however because its lone pair of electrons has been proposed to be responsible for the high ORR-activity in acidic medium.[15, 27, 29-30]

Since it has been shown in the results section that no active sites are leached during the second and subsequent acid-washings of the O-catalyst and that no active sites are created upon re-heat-treatment in argon, the site density, SD, can be assumed constant during the second and also subsequent acid-washings. Hence, the changes in mass activity reflect proportionally-related changes in turnover frequency (see Eq.2 in section 2.2.3). The concept of turnover frequency is used in the remainder of the discussion since it is, at the scale of a single active site, more meaningful than that of the mass activity. While the experimental results demonstrate that protonation of basic N-groups along with anion binding results in a decreased turnover frequency of FeN_4-sites for the ORR, the chemical state of the basic N-groups corresponding to the initial high turnover frequency of FeN_4-sites could be either (i) non-protonated and not anion-bound or (ii) protonated, but not anion-bound. We discuss these two possible cases within the framework of a cathode catalyst in a fully-humidified PEMFC. In either case, the mobility of anions is restricted by their attachment to polymeric chains.

In case (i) an FeN_4-site is assumed to possess high turnover frequency for the ORR as long as nearby basic N-groups remain unprotonated in PEMFC, and switches to the low turnover frequency state when the basic N-groups simultaneously protonate and bind with anions. The time required for the latter is governed by the mobility and speed of polymeric chains in reaching basic N-groups. This scenario would tie in with, and more comprehensively explain, the previously proposed idea of Popov and collaborators that the protonation of pyridinic nitrogen atoms is responsible for the activity decay of non-precious metal catalysts in acidic medium.[15, 29]

In case (ii) an FeN_4-site is assumed to possess high turnover frequency for the ORR as long as nearby basic N-groups are protonated but not anion-bound. This hypothesis implies that protons can swiftly access the basic N-groups in the PEMFC conditions used in this work (fully humidified), while the counter-anions fixed onto polymeric chains do not immediately follow, thus explaining the initially-measured high activity (see reaction scheme on Fig.10, row A, central frame). This protonation event could not have occurred earlier during electrode preparation. When mixing the catalyst powder with the Nafion ionomer solution to form the catalyst ink, the ionomer and catalyst are separated by long distances. Moreover, the solution filling and surrounding the Nafion ionomer is alcohol-based (80-85 %) and has a low dielectric constant, resulting in strong electrostatic interaction between protons and the sulfonate anions fixed onto polymer chains (Coulomb's law). Thus, the distance between protons and their fixed counter-anions is, in these conditions, in the range of angströms; a distance too short to reach the catalyst surface (see later). Protonation of basic N-groups of the catalyst does not occur either when the cathode ink is subsequently dried in a vacuum oven, nor when the anode and cathode are hot-pressed against a Nafion membrane to form a membrane-electrode-assembly, nor when the latter is stored in a dry glove box, as done at

our laboratory. This is because, at all these stages, the low content of water or the fully dry state of the Nafion ionomer ensures that the protons and the polymer-bound sulfonate groups in Nafion are strongly associated by electrostatic interaction. Hence, the protons are not mobile, even at a nanometric scale.

On the other hand, it is possible for protons of the ionomer to reach the catalyst surface in a fully humidified PEMFC cathode, as will be discussed later. In this case, an FeN_4-site would later switch to the low turnover frequency state when, similarly to case (i), polymeric chains slowly approach the NH^+-groups, resulting in anion binding. The latter would form a strong electrostatic interaction NH^+A^-(reaction scheme, row A, right hand side frame) because NH^+ groups are located on the catalyst surface where the dielectric constant of the first layer of water is low (circa 6) compared to that of bulk water (circa 78).[31] Again, according to Coulomb's law, the strength of electrostatic interactions increases when the dielectric constant decreases.

Based on arguments presented below, we believe that hypothesis (ii) is more plausible than hypothesis (i) in a fully-humidified PEMFC. In Nafion ionomer, protons and sulfonate groups are found in hydrophilic nano-channels with a width of circa 4 nm when fully humidified.[32] The precise proton distribution across these nano-channels has been the object of modelling studies.[33-35] For high humidification, the dielectric constant of water in the central part of the channel is expected to reach that of bulk water, while it decreases sharply close to the hydrophobic walls; and the proton concentration behaves similarly.[35] Thus, some protons are found in the channel-axis region and they are circa 2 nm away from sulfonate groups closely attached to the hydrophobic walls. This distance must be compared to that expected between protons of the Nafion ionomer and basic N-groups found on the catalyst surface (including in micropores). In the cathode, the Nafion ionomer is expected to cover the external area of catalytic particles. In contrast to pristine-carbon-black particles, the catalytic particles of the present Fe/N/C-catalyst possess many micropores that penetrate circa 5 nm deep inside the particle.[36] These micropores, etched from the reaction between carbon black and NH_3 during catalyst synthesis, host the FeN_4-moieties and basic N-groups. Thus, on average, the distance between protons from the ionomer covering the external surface of catalytic particles and basic N-groups found in these micropores would be 5 nm/2 = 2.5 nm. Because this distance is comparable to that between protons and sulfonate groups in humidified Nafion (2 nm), some protons from the Nafion ionomer could diffuse inside micropores of the cathode catalyst and protonate their basic N-groups without affecting the electroneutrality of the ionomer phase. This event would occur quickly due to the nanometric distance and high proton mobility in fully humidified conditions.

The protonation of basic N-groups on the cathode-catalyst surface may also occur as soon as the PEMFC generates current. Protons originating from the anode's hydrogen oxidation reaction could protonate basic N-groups at the cathode, instead of participating in the ORR. Consequently, electrons from the anode would accumulate at the cathode-catalyst surface to compensate for the NH^+-groups formed at the catalyst-electrolyte interface. Based on the concentration of basic N-groups determined in this work (value B_0 derived from titration), it is possible to calculate that the charge required to protonate all basic N-groups in this Fe/N/C-based cathode is $3.5\ 10^{-4}$ moles basic N-group/g × 96 450 C/mol = 34 C/g. In comparison, the charge accumulation at the Fe/N/C cathode simply from sweeping the voltage from OCV to 0.8 V in PEMFC during the polarization curve measurement is 300-1000 C/g (Fig. 1B), 10-30 times that required to protonate all basic N-groups of the Fe/N/C-based cathode.

Based on the above two arguments (average proton-to-basic N-group distance and/or charge required for protonation), it seems very likely that these basic N-groups will have protonated soon after current is generated in the PEMFC, supporting hypothesis (ii). Last, a recent study

by Trojanek et al on the homogeneous oxygen reduction catalyzed by a metal-free porphyrin demonstrates the beneficial effect of N-protonation and negative effect of subsequent anion binding on the catalytic activity for ORR,[37] which further supports hypothesis (ii). The work by Trojanek *et al* ties in with our observation that the acid-washing also had an effect for the carbon black pyrolyzed in NH_3 but without adding Fe acetate before the pyrolysis; however the activities for the ORR (before and after acid washing) were always 40-70 times lower than those obtained with the catalyst prepared with the addition of iron acetate (see section 3.2). All these observations support our assertion that the turnover frequency for the ORR is higher when N-groups are protonated but not anion-bound, both on metal-free active sites and FeN_4 sites, with the latter sites being much more active than the former ones.

In conclusion, we propose that protonation of basic N-groups occurs immediately in RDE or fully-humidified PEMFC environment, but that anion binding is delayed in PEMFC due to restricted mobility of the sulfonate groups. Two activity-enhancement effects related to the protonation of neighbouring N-groups and that may be negated by subsequent anion-binding are: (a) modified electron density of the catalyst surface surrounding FeN_4-moieties (i.e. modified oxidation and spin state of the ligated Fe-ion (Refs.38-41)) or (b) increased proton access to FeN_4-centres during the ORR, which requires four protons per oxygen-molecule for the desired complete reduction to water.

Regarding the possible effect (a), a positive correlation between the ORR-activity and electron-withdrawing power of various substituents has been reported for substituted, non-heat-treated metalphthalocyanines or metal-porphyrins (Refs. 38-40), while changes in electron density on the iron atom upon heat-treatment of an Fe-porphyrin have been discussed by Kramm and co-workers.[41]

Regarding the possible effect (b), it must be noted that while protons are already present in the Nafion ionomer, their relative concentration in the micropores of the Fe/N/C-catalysts is unknown. For a PEMFC cathode with known Nafion-ionomer to catalyst mass-ratio (1 in the present work), one can however compare the concentration of SO_3H-groups of the Nafion ionomer with that of protonable N-groups of the catalyst. The former is $9.1 \cdot 10^{-4}$ mol/g_{Nafion} (from the ionomer's equivalent weight of 1100) and the latter is $3.5 \cdot 10^{-4}$ mol/$g_{catalyst}$ (see caption of Fig.8). Hence, in a PEMFC cathode, the amount of protons fixed on specific N-groups is significant, especially if these N-groups are located in micropores, and could play an important role as a relay for the protons migrating from the Nafion ionomer and toward the FeN_4-centres found in the micropores.

Interestingly, a combination of electron-withdrawing effect and nearby presence of proton donor group has recently been shown to increase the ORR activity and selectivity of a xanthene hangman Coporphyrin with a COOH-group suspended above the Co-centre.[40]

Regardless of the exact detailed mechanism (a) or (b) causing the higher turnover frequency of acid-resistant FeN_4-sites upon protonation of basic N-groups, the catalyst is vulnerable to activity decay, the rate of which depends on the pervasiveness of anions in the electrolyte (see reaction scheme). This probably explains why the initial activity of the O-catalyst is much lower when measured in RDE (3 A g^{-1}) compared to that measured in PEMFC (20 A g^{-1}). Indeed, the anion pervasiveness is highest when the O-catalyst powder is subjected directly to the liquid electrolyte during the acid-washing, less so when it is protected from direct contact with anions of the liquid electrolyte by proton-conducting ionomer (RDE-measurement) and least in the PEMFC-measurement where all anions are attached to polymeric chains of the proton-conducting ionomer as sulfonate groups. This might also explain the disparity between initial activities measured in PEMFC and in RDE for other Fe/

N/C-catalysts.[42] This activity decay caused by anion-binding is reversed, in the case of a catalyst powder immersed in acid, by chemical- or heat-treatment (see reaction scheme, B).

The implications of the findings reported in this work are important for the development of highly active and durable Fe/N/C-catalysts for PEMFCs. Combining high activity and durability will require optimizing the catalyst/electrolyte interface to prevent anion-binding. Bearing some similarity to the above problem, it has been shown recently that blocking the close-access of anions to the platinum surface increases the ORR-activity of platinum in strongly-adsorbing acidic electrolytes such as H_2SO_4 or H_3PO_4.[43] It will also be important to investigate in the future if this anion-binding effect also occurs for Fe/N/C-catalysts synthesized using other gases than NH_3 during the pyrolysis (other reacting gases such as CO_2, or inert gas). While, for the sake of clarity, the active sites of the presently investigated catalyst have been labelled simply as FeN_4, there is evidence from previous reports that at least two different active sites corresponding to this formula exist, i.e. FeN_4 sites embedded in, or placed above, a single graphene sheet and FeN_{2+2} sites situated in a micropore defined by two adjacent graphene sheets.[44-46] Different behaviours or magnitudes with regard to the presently unravelled anion-binding effect could therefore be observed with different Fe/- or Co/N/C catalysts.

5. Conclusions

5.1. The effect of a post-synthesis acid-washing on the active sites, chemistry of the catalytic surface and activity for the oxygen electro-reduction was investigated for an Fe/N/C catalyst prepared by the impregnation method and subsequent pyrolysis in NH_3 [20] by various techniques (Mössbauer spectroscopy, EXAFS, TOFSIMS, XPS, titration).

5.2. The acid-washing results, for this specific Fe/N/C-catalyst, in a one-order-of-magnitude decay of its activity for the ORR.

5.3. It is revealed that half of this activity decay can be recovered ex-situ either chemically or thermally at 400°C in Argon; a temperature at which no new active sites can be formed.

5.4. The activity recovery coincides with the removal of anions that bound on the surface during the acid-washing.

5.5. This recoverable activity decay is ascribed to acid-resistant FeN_4-sites (and more precisely, FeN_{2+2} sites situated in micropores) whose turnover frequency for the ORR is tuned by the chemical state of basic N-groups on the catalytic surface; high when the basic N-groups are protonated but not yet anion-bound, and low once anions have neutralized the protonated basic N-groups.

5.6. It is inferred from these ex-situ characterizations and catalytic reactivation methods that slow anion binding by polymeric anions is most probably the reason for the large activity decay with time observed on this specific Fe/N/C-catalyst in PEMFC under conditions where no oxygen reduction occurs. Preventing anion binding in PEMFC could thus solve this type of activity decay.

Supplementary Material

Refer to Web version on PubMed Central for supplementary material.

Acknowledgments

The authors acknowledge the support of NSERC, General Motors of Canada and MDEIE of the Québec Government, thank the Sid Richardson Carbon Corporation and Cabot for providing the carbon blacks and are

grateful to C. Poleunis for his help with Time-of-flight Secondary-ion Mass-spectrometry measurements and to T. Scherb for access to the thermogravimetry-spectrometry system. The authors are also grateful for the use of X3-B at the National Synchrotron Light Source, Brookhaven National Laboratory, which is supported by the U.S. Department of Energy, Office of Science, Office of Basic Energy Sciences, under contract No. DE-AC02-98CH10886.

References

1. James BD, Kalinoski JA, U.S. DOE. 2008 Annual progress report: Fuel Cells.
2. Gasteiger HA, Panels JE, Yan SG. J Power Sources. 2004; 127:162–171.
3. Jasinski R. Nature. 1964; 201:1212–1213.
4. Bagotzky VS, Tarasevich MR, Radyushkina KA, Levina OE, Andrusyova SI. J Power Sources. 1977; 2:233–240.
5. Gupta SL, Tryk D, Bae I, Aldred W, Yeager EB. J Appl Electrochem. 1989; 19:19–27.
6. Wang H, Côté R, Faubert G, Guay D, Dodelet JP. J Phys Chem B. 1999; 103:2042–2049.
7. Dodelet, JP. Oxygen reduction in PEM fuel cell conditions: heat-treated non-precious metal-N4 macrocycles and beyond. In: Zagal, JH.; Bedioui, F.; Dodelet, JP., editors. N_4-Macrocyclic Metal Complexes. Springer Science + Business Media Inc.; New-York: 2006. p. 83-150.
8. Joyner RW, van Veen JAR, Sachtler WMH. J Chem Soc, Faraday Trans 1. 1982; 78:1021–1028.
9. Bouwkamp-Wijnoltz AL, Visscher W, van Veen JAR, Tang SC. Electrochim Acta. 1999; 45:379–386.
10. Bron M, Radnik J, Fieber-Erdmann M, Bogdanoff P, Fiechter S. J Electroanal Chem. 2002; 535:113–119.
11. Koslowski UI, Abs-Wurmbach I, Fiechter S, Bogdanoff P. J Phys Chem C. 2008; 112:15356–15366.
12. Lefevre M, Dodelet JP, Bertrand P. J Phys Chem B. 2000; 104:11238–11247.
13. Lefevre M, Proietti E, Jaouen F, Dodelet JP. Science. 2009; 324:71–74. [PubMed: 19342583]
14. Lalande G, Côté R, Guay D, Dodelet JP, Weng LT, Bertrand P. Electrochim Acta. 1997; 42:1379–1388.
15. Liu G, Li X, Popov BN. ECS Transactions. 2009; 25:1251–1259.
16. Wu G, Artyushkova K, Ferrandon M, Kropf AJ, Myers D, Zelenay P. ECS Transactions. 2009; 25:1299–1311.
17. Wu G, More KL, Johnston CM, Zelenay P. Science. 2011; 332:443–447. [PubMed: 21512028]
18. Baranton S, Coutanceau C, Roux C, Hahn F, Leger JM. J Electroanal Chem. 2005; 577:223–234.
19. Gouerec P, Biloul A, Contamin O, Scarbeck G, Savy M, Riga J, Weng LT, Bertrand P. J Electroanal Chem. 1997; 422:61–75.
20. Jaouen F, Lefèvre M, Dodelet JP, Cai M. J Phys Chem B. 2006; 110:5553–5558. [PubMed: 16539496]
21. Jaouen F, Dodelet JP. Electrochim Acta. 2007; 52:5975–5984.
22. Lefevre M, Dodelet JP. Electrochim Acta. 2003; 48:2749–2760.
23. Herranz J, Lefevre M, Larouche N, Stansfield B, Dodelet JP. J Phys Chem C. 2007; 111:19033–19042.
24. Kang, ET.; Neoh, KG.; Tan, KL. Advances in Polymer Science. Springer-Verlag; Heidelberg: 1993. p. 135-190.
25. Debrunner, PG. Iron Porphyrins Part III. Lever, ABP.; Gray, HB., editors. VCH; New York: 1989. p. 139-234.
26. Thorum MS, Hankett JM, Gewirth AA. J Phys Chem Lett. 2011; 2:295–298.
27. Wood T, Atanasoski R, Schmoeckel AK. US patent number WO 2008/127828 A1. 2008
28. Williams, R. http://research.chem.psu.edu/brpgroup/pKa_compilation.pdf
29. Liu G, Li X, Ganesan P, Popov BN. Appl Catal B:Environ. 2009; 93:156–165.
30. Biddinger EJ, Ozkan US. J Phys Chem C. 2010; 114:15306–15314.

31. Bockris, JO'M.; Reddy, AKN. Modern electrochemistry. Vol. 2. Plenum Press; New York: 1970. p. 756
32. Malek K, Eikerling M, Wang Q, Liu Z, Otsuka S, Akizuki K, Abe M. J Chem Phys. 2008; 129:204702. [PubMed: 19045874]
33. Eikerling M, Kornyshev AA. J Electroanal Chem. 2001; 502:1–14.
34. Paul R, Paddison SJ. J Chem Phys. 2005; 123:224704. [PubMed: 16375492]
35. Kreuer KD, Paddison SJ, Spohr E, Schuster M. Chem Rev. 2004; 104:4637–4678. [PubMed: 15669165]
36. Jaouen F, Dodelet JP. J Phys Chem C. 2007; 111:5963–5970.
37. Trojanek A, Langmaier J, Sebera J, Zalis S, Barbe JM, Girault HH, Samec Z. Chem Commun. 2011; 47:5446–5448.
38. Zagal JH, Gulppi M, Isaacs M, Cardenas-Jiron G, Aguirre MJ. Electrochim Acta. 1998; 44:1349–1357.
39. Baker R, Wilkinson DP, Zhang J. Electrochim Acta. 2008; 53:6906–6919.
40. McGuire R, Dogutan DK, Teets TS, Suntivich J, Shao-horn Y, Nocera DG. Chem Sci. 2010; 1:411–414.
41. Kramm UI, Abs-Wurmbach I, Herrmann-Geppert I, Radnik J, Fiechter S, Bogdanoff P. J Electrochem Soc. 2011; 158:B69–B78.
42. Jaouen F, et al. Appl Mater Interf. 2009; 1:1623–1639.
43. Strmcnik D, Kodama K, van der Vliet D, Greeley J, Stamenkovic VR, Markovic NM. Nat Chem. 2010; 2:880–885. [PubMed: 20861905]
44. Charreteur F, Jaouen F, Ruggeri S, Dodelet JP. Electrochim Acta. 2008; 53:2925–2938.
45. Herranz J, Jaouen F, Dodelet JP. Electrochem Soc Trans. 2009; 25(1):117–128.
46. Bouwkamp-Wijnoltz AL, Visscher W, van Veen JAR, Boellaard E, van der Kraan AM, Tang SC. J Phys Chem B. 2002; 106:12993–13001.

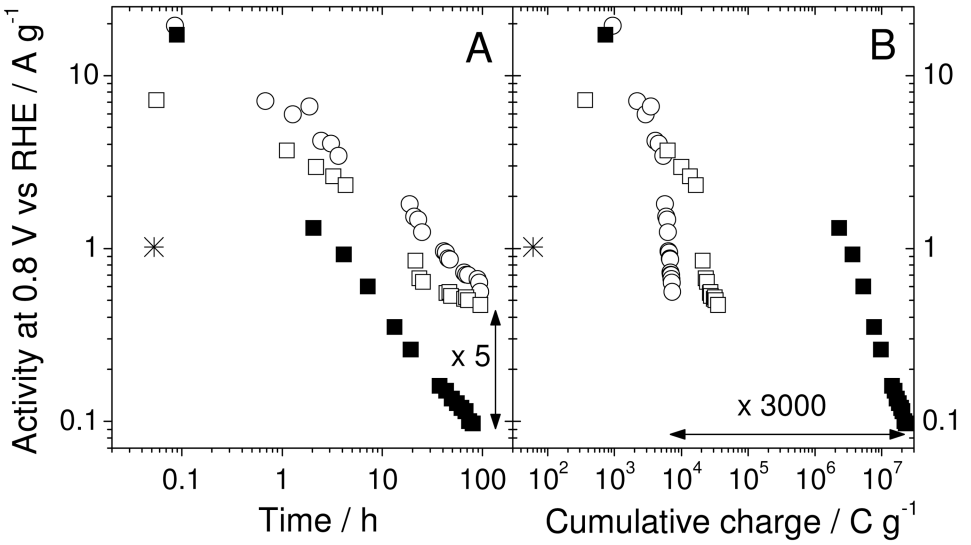

Figure 1. ORR-activity in PEMFC vs. time or cumulative charge

(A) ORR-activity of the original catalyst vs. time using the OCV-Mode (hollow circles) or 0.5V-Mode under N_2 (hollow squares) or 0.5V-Mode under O_2 (filled squares). The asterisk is the initial activity of the acid-washed catalyst obtained after acid washing the original catalyst in a pH 1 H_2SO_4-solution for 100 h, then filtering, rinsing with deionized water and drying.

(B) Same as (A) except that the ORR-activity is plotted vs. the cumulative Faradaic charge.

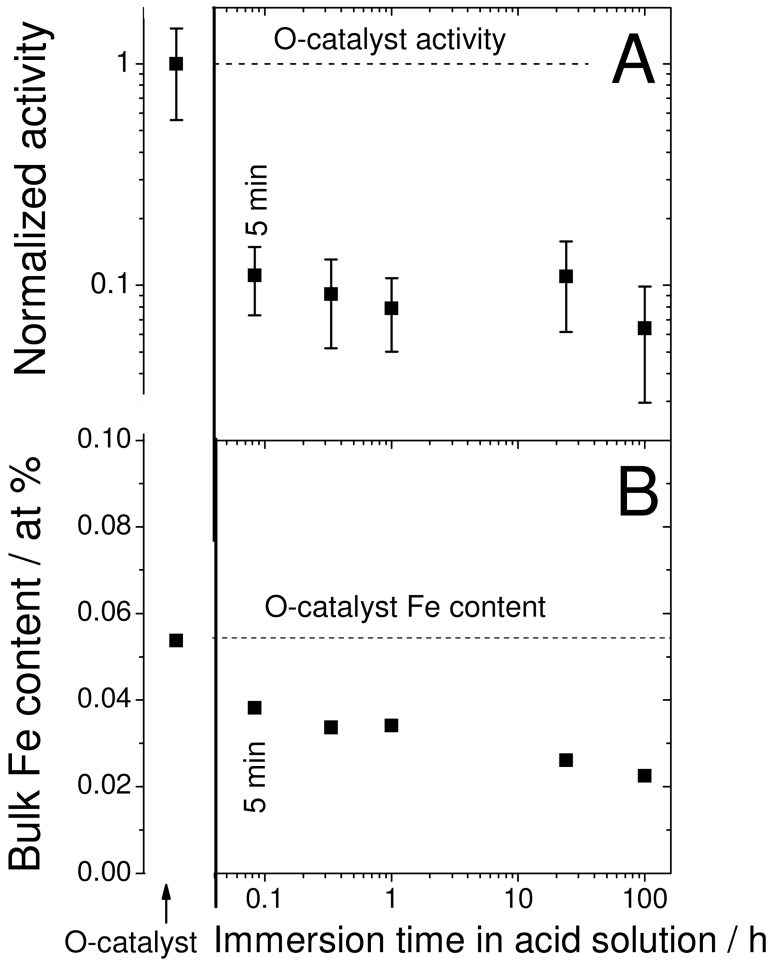

Figure 2. Normalized ORR-activity and bulk iron content of acid-washed catalysts vs. immersion time in a pH 1 H_2SO_4-solution

(A) The original catalyst (O-catalyst) was immersed for a time t (x-axis) in a pH 1 H_2SO_4-solution, then filtered, rinsed with deionized water and dried overnight in an oven at 80°C. Then, an ink was made with the acid-washed catalyst, an aliquot of the ink was deposited on the glassy carbon and the activity measured by RDE in a pH 1 H_2SO_4-electrolyte. The normalized activity is based on that of the original catalyst, which was 2.8 ± 0.6 Ag^{-1}.
(B) The bulk iron content was measured by neutron activation analysis and the error is 5 %.

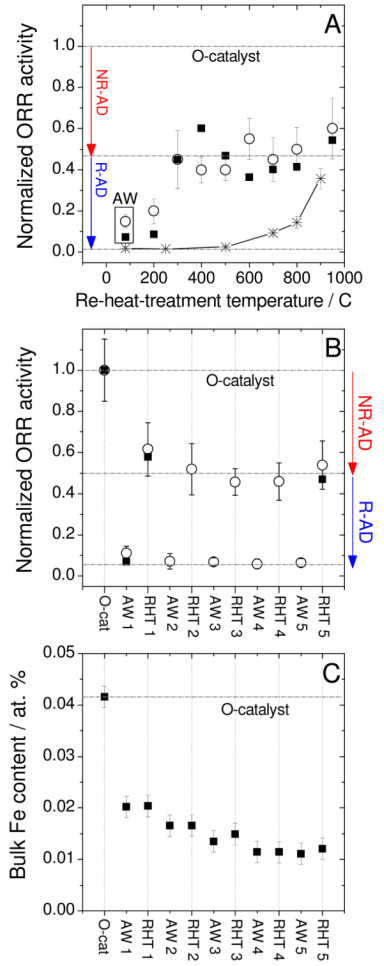

Figure 3. Activity recovery by re-heat-treatment in argon of acid-washed catalysts

(A) Normalized activity based on that of the original catalyst (O-catalyst) vs. re-heat-treatment temperature in argon, as measured in RDE (open circles) and PEMFC (filled squares).

The acid-washing was performed in a pH 1 H_2SO_4-solution for 24 h, then the powder was filtered, rinsed with deionized water and dried. Several aliquots of the acid-washed catalyst (AW-catalyst) were re-heat-treated in argon at various temperatures for 1 h. The initial activities of the O-catalyst were 2.8 and 15.1 A g^{-1} in RDE and PEMFC, respectively. Aliquots of a test precursor initially free of active sites (see section 2.1.4) were heat-treated in argon at various temperatures for 1 h (asterisks) in order to determine the minimum temperature required for catalytic-site formation.

(B) Normalized activity as measured in RDE (open circles) or PEMFC (filled squares) at various steps of five successive acid-washing/re-heat-treatment cycles. Acid-washed and re-heat-treated catalysts are labeled AWX and RHTX, respectively, X denoting the cycle number. Each acid-washing lasted 24 h in a pH 1 H_2SO_4-solution, then the powder was filtered, rinsed and dried. Each AW-catalyst was re-heat-treated for 1 h at 950°C in argon.

(C) Bulk Fe content at each step of the five acid-washing/re-heat-treatment cycles described in (B), as measured by neutron activation analysis.

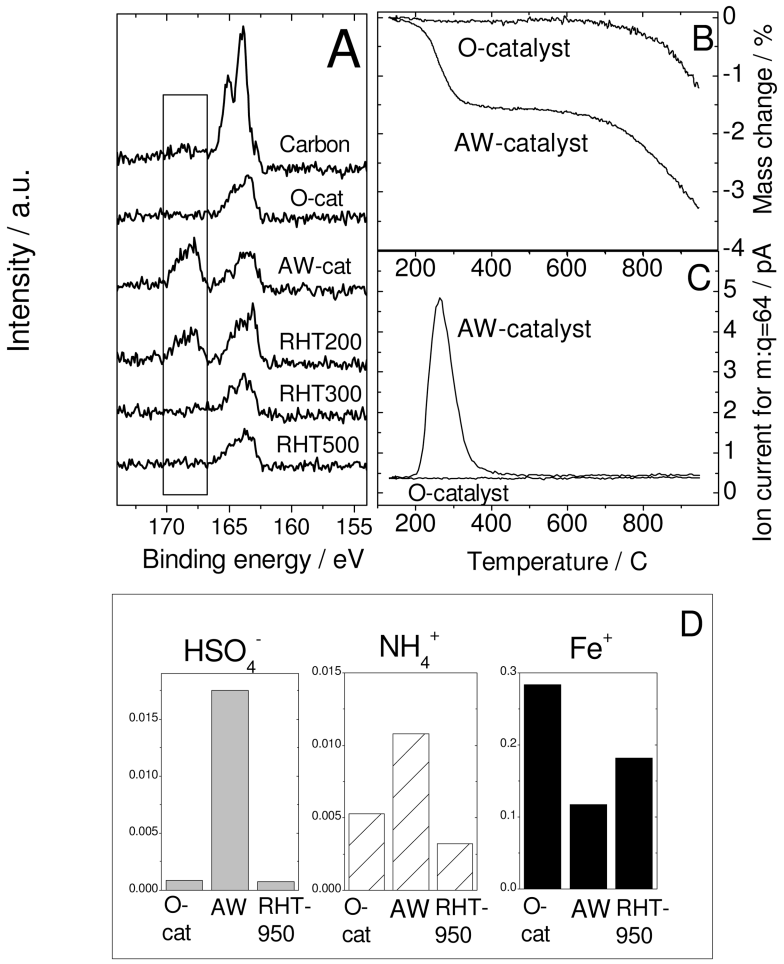

Figure 4. Identification of surface species linked to activity decay

(A) X-ray photo-electron spectra of S_{2p} for the pristine carbon black (label "carbon") used to synthesize the original catalyst (O-cat), acid-washed catalyst (AW-cat) and aliquots of the latter re-heat-treated in argon for 1 h at 200, 300 or 500°C (RHT200, RHT300, RHT500, respectively).

(B) Thermogravimetry using a heating rate of 10 K min^{-1} and under argon flow of the O-catalyst and AW-catalyst.

(C) Ion mass-spectrometry for m:q = 64 (assigned to SO_2) that was acquired simultaneously with the thermogravimetry shown in (B).

(D) Time-of-flight secondary-ion mass-spectrometry detecting HSO_4^-, NH_4^+ and Fe^+ ions emitted from the top-surface layer of the O-catalyst, AW-catalyst and AW-catalyst re-heat-treated at 950°C for 1 h in argon (RHT950).

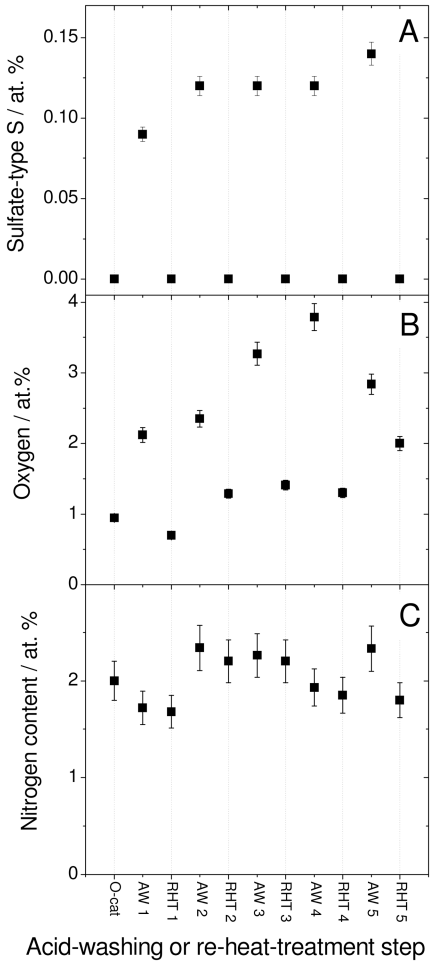

Figure 5. Sulfate-type S, O and N contents measured by XPS at various steps of five acid-washing/re-heat-treatment cycles

Acid-washed and re-heat-treated catalysts are labeled AWX and RHTX, respectively, × denoting the cycle number. Each acid-washing lasted 24 h in a pH 1 H_2SO_4-solution, then the powder was filtered, rinsed and dried. Each AW-catalyst was re-heat-treated for 1 h at 950°C in argon.

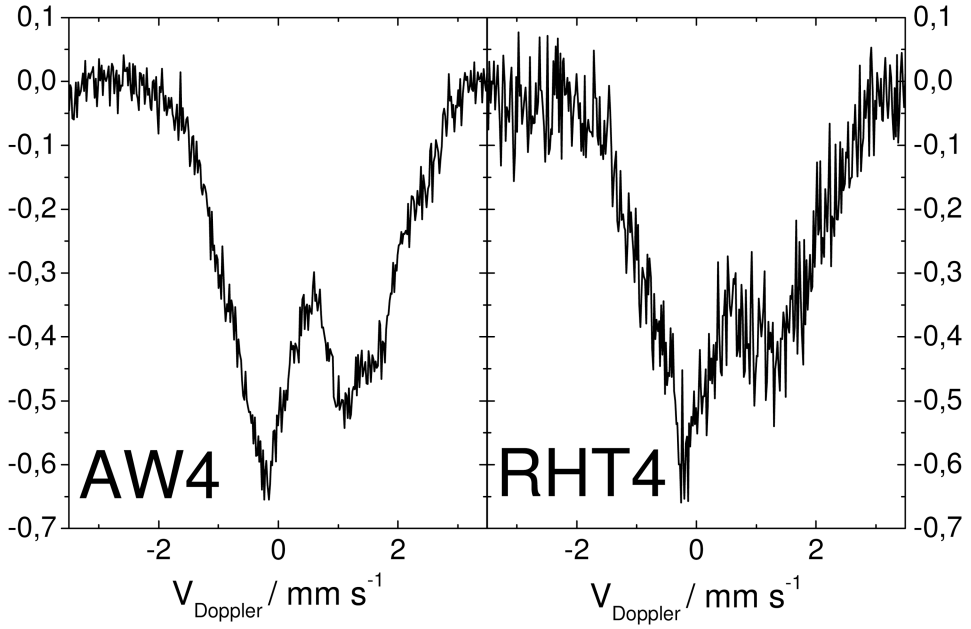

Figure 6. Mössbauer Spectroscopy for an acid-washed (AW4) and a re-heat-treated (RHT4) catalyst from the fourth acid-washing/re-heat-treatment cycle

Each acid-washing lasted 24h in a pH 1 H_2SO_4-solution, then the powder was filtered, rinsed and dried. Each re-heat-treatment lasted 1 h at 400°C in argon. This temperature of 400°C is lower than that used for the re-heat-treatment in Fig.3B (950°C in argon), however the resulting activities for the re-heat-treated catalysts are the same (Fig.3A). The data were acquired for several weeks in order to minimize the noise.

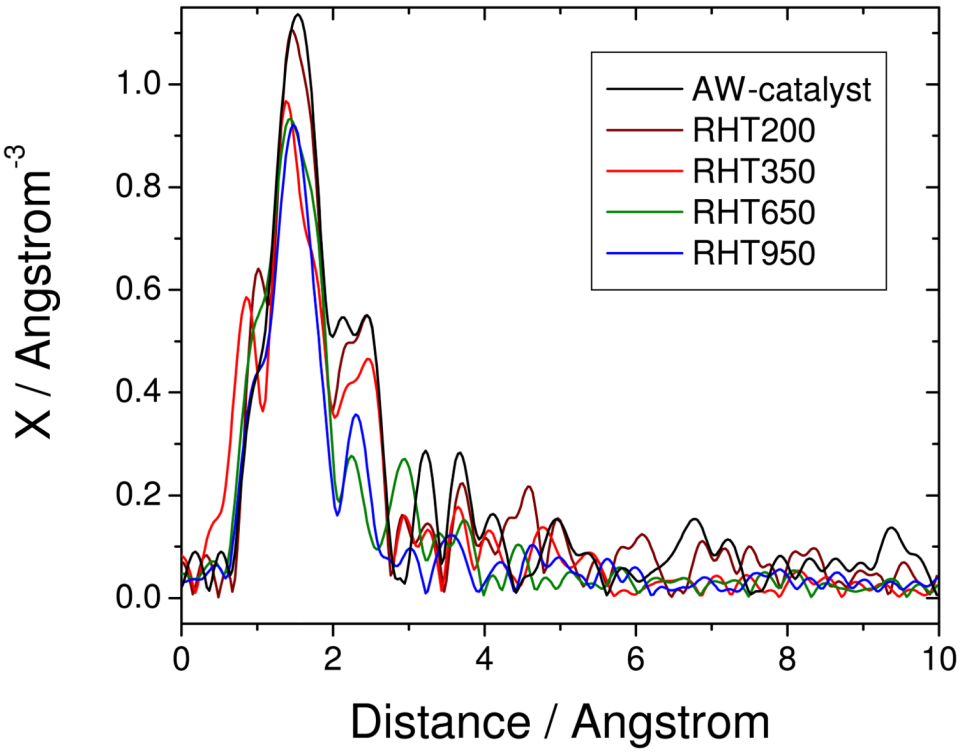

Figure 7. Fourier-transformed EXAFS-spectra of the acid-washed catalyst (AW-catalyst) and of selected re-heat-treated catalysts (RHT-catalysts)

The AW-catalyst was re-heat-treated in argon at various temperatures, resulting in re-heat-treated catalysts (RHT, followed by the three-digits indicating the heat-treatment temperature). The spectra are not corrected for phase shift and the true distances corresponding to each peak are obtained from these uncorrected spectra only after a correction that depends on the peak assignment.

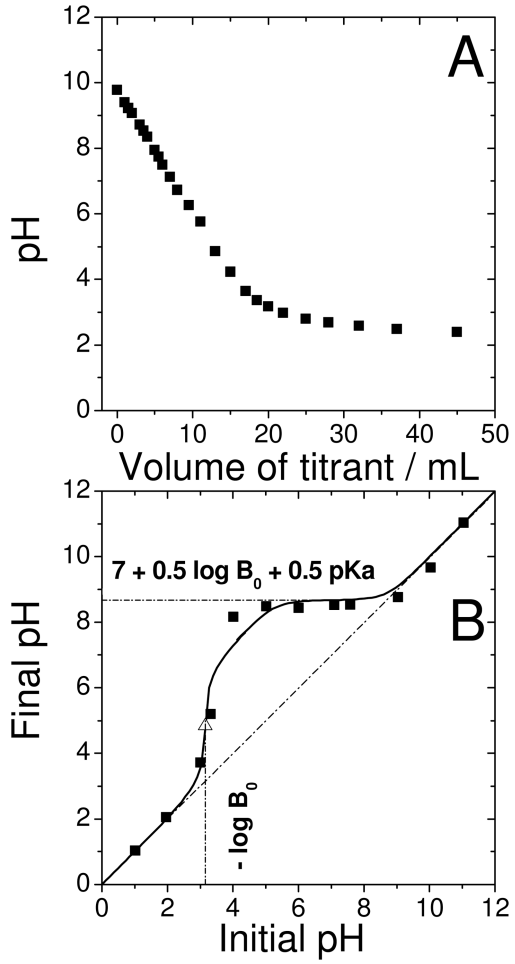

Figure 8. Investigation of basic groups on the catalyst surface by classical and Boehm titration

(A) Classical titration: 500 mg of the original catalyst was dispersed in 25 mL of deionized water and 250 μL ethanol, then the solution was titrated by a 0.01 M aqueous solution of $HClO_4$.

(B) Boehm titration: The original catalyst was divided into several aliquots of 20 mg and each was immersed for 20 min in 10 mL-solution of a given initial pH, then the final pH was measured (filled squares in B). The solutions were dilute aqueous solutions of either H_2SO_4 or NaOH.

A calculated curve corresponding to a concentration of basic groups B_0 from the catalyst of $7 \cdot 10^{-4}$ mol L^{-1} (equivalent to $7 \cdot 10^{-4}$ mol L^{-1} × 10mL/20mg = $3.5 \cdot 10^{-4}$ mol per gram catalyst) with pKa of 6.5 is also shown (solid line in (B)). In the equation, log is the base-ten logarithm function. The calculated inflection point (equivalence point) is indicated by the open triangle

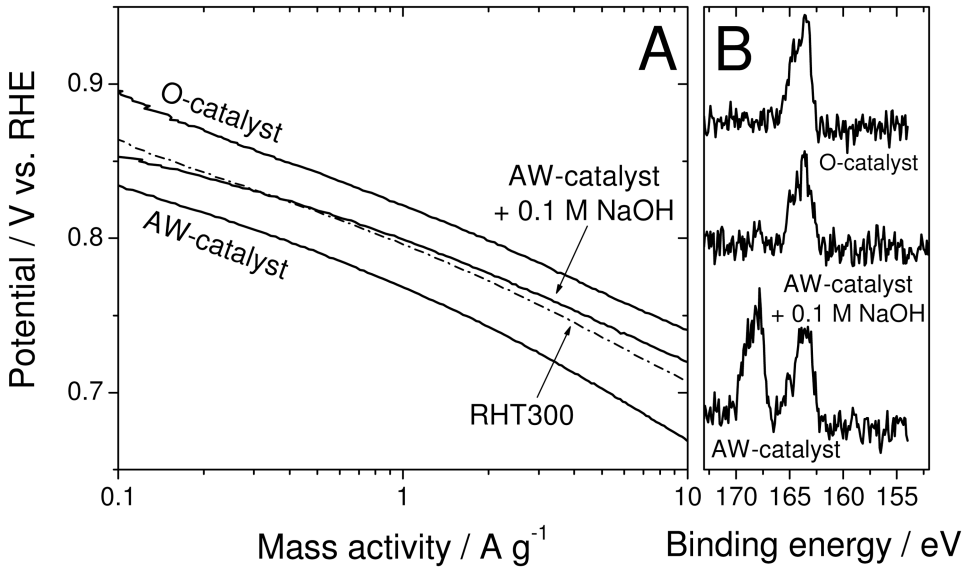

Figure 9. Chemical activity-recovery

(A) Tafel plots derived from RDE-voltammetry in pH 1 H_2SO_4-solution for four catalysts: (i) O-catalyst, (ii) AW-catalyst obtained by acid washing the O-catalyst in 0.1 M H_2SO_4, filtering, rinsing and drying, (iii) a chemically-reactivated catalyst obtained by acid-washing the O-catalyst, filtering, base-washing the filtrate in 0.1 M NaOH, rinsing and drying, and (iv) the AW-catalyst re-heat-treated in Ar at 300°C.

(B) X-ray photo-electron spectra of S_{2p} for the O-catalyst, AW-catalyst and chemically reactivated catalyst

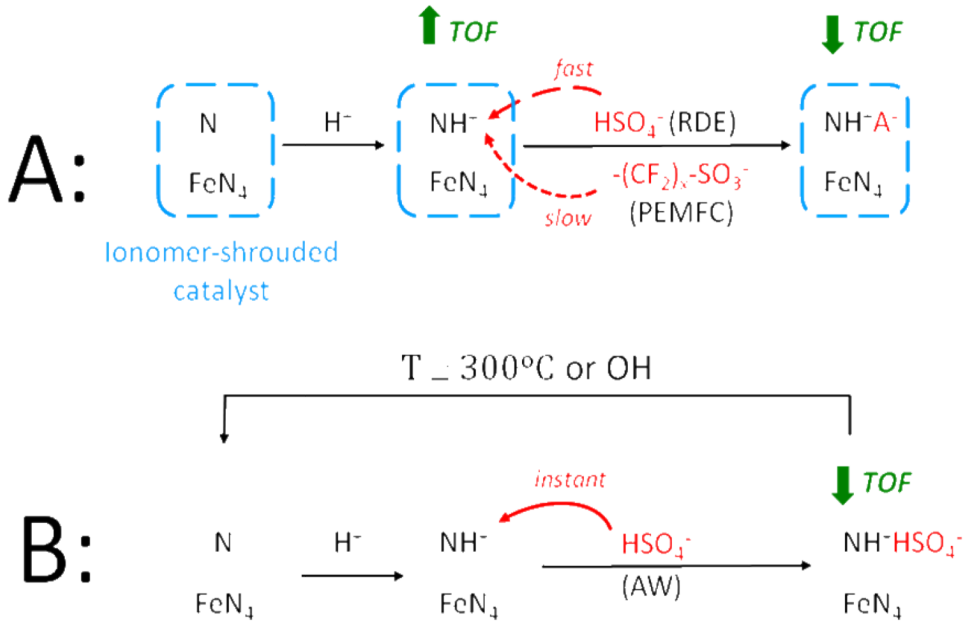

Figure 10. (scheme)

Change of the chemical state of protonable N-groups and simultaneous change of the turnover frequency (TOF) for the ORR of FeN_4 catalytic sites when the Fe/N/C-catalyst is shrouded by proton-conducting ionomer (A) or directly in contact with an aqueous acidic solution (B). In case (B), the acid-washed catalyst can be reactivated either thermally or chemically. This scheme applies to Fe/N/C-catalysts obtained after a pyrolysis in NH_3 with active sites labeled here as FeN_4 for simplicity, but which have also been labeled as FeN_{2+2} previously to highlight the fact that they are hosted in micropores.[44-45]